Available online at www.sciencedirect.com

ScienceDirect

Journal of the European Ceramic Society 30 (2010) 3087–3092

www.elsevier.com/locate/jeurceramsoc

Stability of the δ-TeO_2 phase in the binary and ternary TeO_2 glasses

A.E. Ersundu [*], G. Karaduman, M. Çelikbilek, N. Solak, S. Aydin

Istanbul Technical University, Department of Metallurgical and Materials Engineering, Istanbul 34469, Turkey

Received 12 February 2010; accepted 8 July 2010

Available online 3 August 2010

Abstract

The stability of δ-TeO_2 phase was studied in binary TeO_2–WO_3, TeO_2–CdO and ternary TeO_2–WO_3–CdO glasses. The samples were prepared by heating high purity powder mixtures of TeO_2, WO_3 and/or CdO to 800 °C in a platinum crucible with a closed lid, holding for 30 min and quenching in water bath. Differential thermal analysis (DTA), X-ray diffraction (XRD) and scanning electron microscopy (SEM) techniques were used to characterize the thermal, phase and microstructural properties of the δ-TeO_2 phase. The addition of CdO into the tellurite glasses increased the stability range of the δ-TeO_2 phase up to higher temperature values and expanded the compositional δ-TeO_2 formation range. The formation of δ-TeO_2 phase in the binary systems was observed for samples containing 5–10 mol% WO_3 and 5–15 mol% CdO. However, for the ternary TeO_2–WO_3–CdO system the formation of δ-TeO_2 phase was determined in a wider compositional range.

Keywords: δ-TeO_2; Glass; Thermal properties; Microstructure-final

1. Introduction

Comparing with silicate, borate and phosphate glasses, tellurite glasses have superior properties, such as low-phonon energy, high linear and non-linear refractive index, high dielectric constant, thermal and chemical stability. Therefore, considerable attention has been focused on tellurite based glasses for their potential use in fiber optics, laser hosts and non-linear optical materials.[1–7] TeO_2 is a conditional glass former which does not transform to the glassy state under normal quenching conditions. Therefore, addition of a secondary component such as heavy metal oxides, alkalis or halogens increases the glass forming ability.[7]

TeO_2 is known to exist in two polymorphs at ambient conditions: tetragonal α-TeO_2 (paratellurite) and orthorhombic β-TeO_2 (tellurite).[1] Blanchandin et al.[2] determined two new metastable polymorphs of TeO_2, namely orthorhombic γ-TeO_2 and cubic δ-TeO_2, which were obtained in the doped TeO_2 glasses, depending on the amount of the added component. The formation of δ-TeO_2 phase under special quenching conditions was reported in several studies on tellurite based binary glass systems[2–5] by a research group and under normal quenching conditions on a ternary glass system[6] by another group. However, no studies exist solely on the formation of δ-TeO_2 phase in binary and ternary tellurite systems.

The δ-TeO_2 polymorph was first detected for samples containing about 5–10 mol% WO_3, however the preparation of this metastable phase from pure TeO_2 glassy samples was unsuccessful.[2] In another study about the TeO_2–Nb_2O_5 system, Blanchandin et al.[3] observed δ-TeO_2 phase, for samples in the range 2.5–12.5 mol% Nb_2O_5. Mirgorodsky et al.[4] analyzed the Raman spectra of δ-TeO_2 phase, which was detected in samples containing a little amount of WO_3 (5–10 mol%) and claimed that the δ-TeO_2 phase is an intermediate structure between the crystalline and glass states. Noguera et al.[5] reported that the Raman spectrum of δ-TeO_2 shows no difference comparing to the spectrum of the glass. Lastly, Tatar et al.[6] observed δ-TeO_2 phase in the ternary TeO_2–CdF_2–WO_3 glass system for different compositions, however did not report the formation of δ-TeO_2 phase in the binary TeO_2–WO_3 and TeO_2–CdF_2 systems.

The present study, which is part of an ongoing research on tellurite based systems, aims to investigate the formation of δ-TeO_2 phase in the TeO_2-rich part of the binary TeO_2–WO_3, TeO_2–CdO and ternary TeO_2–WO_3–CdO glasses by applying thermal and microstructural characterizations.

---

[*] Corresponding author. Tel.: +90 212 285 72 03; fax: +90 212 285 34 27.
E-mail address: ersundu@itu.edu.tr (A.E. Ersundu).

0955-2219/$ – see front matter © 2010 Elsevier Ltd. All rights reserved.
doi:10.1016/j.jeurceramsoc.2010.07.018

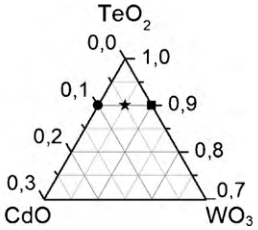

Fig. 1. Compositions of the prepared samples, where (■) TW10, (●) TC10, (⋆) TW5C5.

2. Experimental procedure

In the experimental studies, samples were prepared with different amounts of WO_3 and CdO by keeping TeO_2 content constant at 90% in molar ratio. Therefore, three different samples with the compositions of $0.90TeO_2$–$0.10WO_3$, $0.90TeO_2$–0.10CdO and $0.90TeO_2$–$0.05WO_3$–0.05CdO (now hereafter referred to as the TW10, TC10 and TW5C5 glasses, respectively) were obtained as shown in Fig. 1.

High purity raw materials of TeO_2 (99.99% purity, Alfa Aesar Company), WO_3 (99.8% purity, Alfa Aesar Company) and CdO (99.95% purity, Alfa Aesar Company) were used to prepare the samples. The powder batches of 5 g size were thoroughly mixed in an agate mortar and melted in a platinum crucible with a closed lid at 800 °C for 30 min to provide complete homogeneity of the melts. Afterwards, the molten samples were removed from the furnace and quenched in water bath and thermal characterization experiments were realized by using differential thermal analysis (DTA) technique. DTA scans of the samples were carried out in a Perkin Elmer^{TM} Diamond TG/DTA to determine the glass transition and crystallization temperatures. The glass transition onset temperatures (T_g) were taken as the inflection point of the endothermic change of the calorimetric signal. Onset temperatures were specified as the beginning of the reaction where the crystallization or melting first starts and peak temperatures represent the maximum value of the exotherm or endotherm. The DTA scans were recorded by using 25 mg powdered samples. All thermal analyses were realized with a heating rate of 10 K/min from room temperature to 550 °C in a platinum crucible in a flowing (100 ml/min) argon gas. According to the DTA results, as-cast samples were heat-treated for 24 h above the first and second exothermic onset temperatures for each composition in order to achieve the thermal equilibrium of these crystalline phases. Afterwards, X-ray diffraction (XRD) analyses were carried out on as-cast and heat-treated samples to determine the crystalline phases and scanning electron microscopy (SEM) studies were conducted for microstructural characterization. The X-ray diffraction investigations were carried out with powdered samples in a Bruker^{TM} D8 Advanced Series powder diffractometer using Cu K_α radiation in the 2θ range from 10° to 90°. The International Centre for Diffraction Data (ICDD) files were used to determine the crystallized phases by comparing the peak positions and intensities. SEM investigations were conducted with platinum-coated bulk samples in JEOL^{TM} Model JSM 7000F operated at 15 kV and linked with Oxford Inca energy dispersive X-ray spectrometer (EDS) attachment.

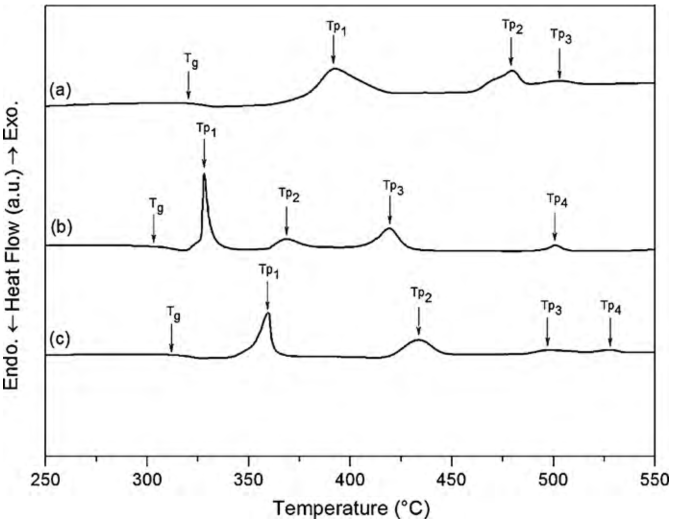

Fig. 2. DTA curves of as-cast (a) TW10, (b) TC10 and (c) TW5C5 samples.

3. Results and discussion

3.1. Thermal analyses

DTA curves of as-cast TW10, TC10 and TW5C5 samples are given in Fig. 2. In general, DTA scans show a glass transition and several exothermic peaks corresponding to the crystallization and transformation of different crystalline phases. The glass transition onset (T_g), crystallization onset and peak (T_c/T_p) temperature values are listed in Table 1.

As can be seen from Fig. 2, an endothermic change between 304 and 320 °C corresponding to the glass transition temperature (T_g) was observed for all compositions indicating the glassy nature of the as-cast samples. For TC10 sample, the glass transition onset temperature was determined at 304 °C, while in WO_3 containing samples (TW10 and TW5C5) the glass transition was detected at higher temperatures. Therefore, by comparing the glass transition temperatures for all three samples, it can be concluded that the addition of WO_3 into TeO_2 based glasses shifts the glass transition temperature to higher values, which is in agreement with literature.[2,7] However, the difference between T_g and T_{c1}, i.e. $\Delta T = T_{c1} - T_g$, indicating the thermal stability against crystallization were found to be 53 °C and 39 °C for TW10 and TW5C5 samples, respectively is higher than TC10 sample showing a ΔT value of 23 °C.

Several exothermic peaks indicating different crystallization steps were determined at higher temperatures. Four crystallization steps were determined for TC10 and TW5C5 samples, while TW10 sample showed three crystallization steps. However, for TW10 sample, the first broad exothermic peak indicates the crystallization of three phases occurring at the same temperature interval so that only one large exothermic peak was observed.

3.2. XRD results

On the basis of the DTA results, X-ray diffraction analyses were conducted on as-cast and heat-treated samples. XRD patterns of the as-cast samples are given in Fig. 3.

Table 1
Values of glass transition onset, T_g, crystallization onset, T_c, crystallization peak, T_p, thermal stability against crystallization, ΔT, temperatures of the as-cast samples.

Samples	T_g (°C)	T_{c1}/T_{p1} (°C)	T_{c2}/T_{p2} (°C)	T_{c3}/T_{p3} (°C)	T_{c4}/T_{p4} (°C)	$\Delta T = T_{c1} - T_g$ (°C)
TW10	320	373/397	466/482	495/507		53
TC10	304	327/333	358/368	409/420	495/501	23
TW5C5	313	352/360	420/433	488/497	–/528	39

–, undetermined values.

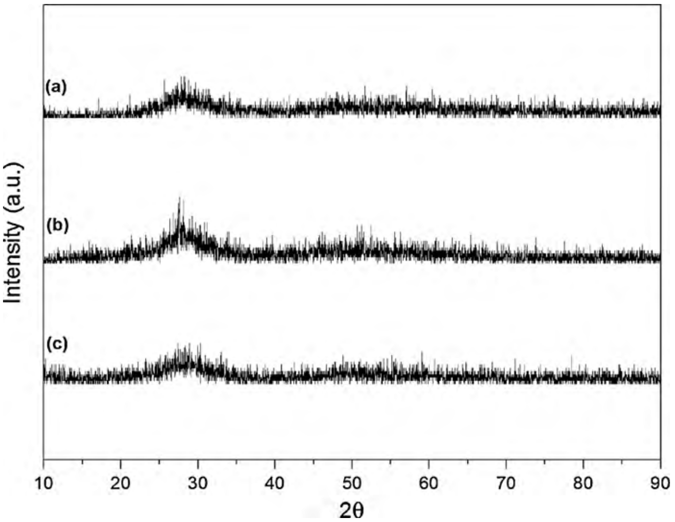

Fig. 3. X-ray diffraction patterns of as-cast (a) TW10, (b) TC10, (c) TW5C5 samples.

As can be seen from Fig. 3, XRD patterns of the as-cast samples revealed no detectable peaks, proving the amorphous glassy structure of the as-cast samples. Therefore, as-cast samples were heat-treated for 24 h above the first crystallization onset temperatures for each composition in order to obtain the first crystalline phases. 390 °C, 335 °C and 365 °C were selected as annealing temperatures for TW10, TC10 and TW5C5 samples, respectively. XRD patterns of the heat-treated samples above the first crystallization onset temperatures are shown in Fig. 4.

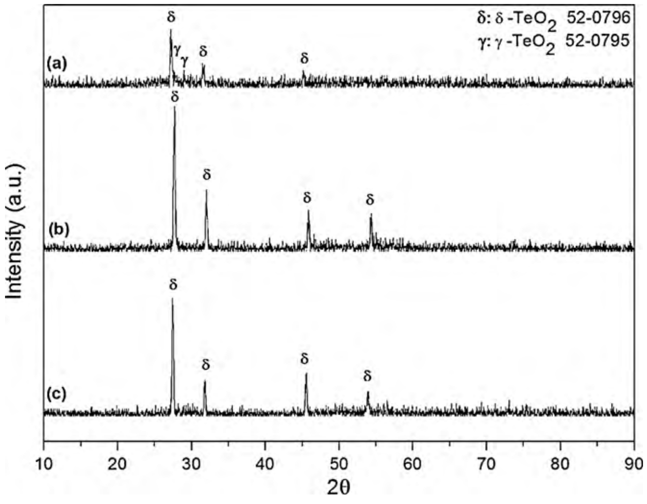

Fig. 4. X-ray diffraction patterns of heat-treated samples for 24 h (a) TW10 at 390 °C, (b) TC10 at 335 °C, (c) TW5C5 at 365 °C.

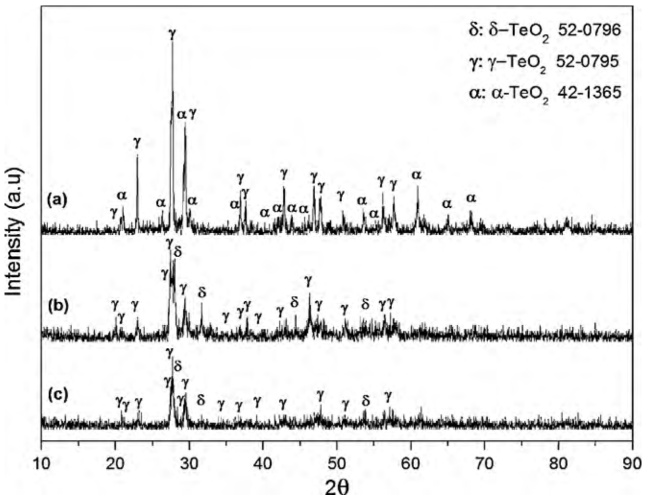

Fig. 5. X-ray diffraction patterns of heat-treated samples for 24 h (a) TW10 at 410 °C, (b) TC10 at 370 °C and (c) TW5C5 at 435 °C.

It can be seen in Fig. 4a, for TW10 sample heat-treated at 390 °C for 24 h, the peak intensities of the crystalline phases are weak due to the amorphous nature of the background. A good match was found between the observed peak positions and card values of two metastable phases, namely δ-TeO_2 which has a cubic crystal structure and γ-TeO_2 which has orthorhombic crystal structure.[2] On the other hand, as seen in Fig. 4b and c, X-ray investigations on the TC10 and TW5C5 samples heat-treated for 24 h at 335 °C and 365 °C, respectively revealed only the formation of δ-TeO_2 phase. δ-TeO_2 phase was detected for the first time in the literature for TC10 and TW5C5 glasses.

In order to obtain a better understanding on the transformation behavior of the metastable δ-TeO_2 phase, as-cast samples were heat-treated for 24 h above the second crystallization onset temperatures. However, for TW10 sample due the broad nature of the first exothermic peak, which indicates three crystallization mechanisms occurring at the same temperature interval, the sample was heat-treated above the first exothermic peak temperature. XRD patterns of the heat-treated samples above the second crystallization onset temperatures are given in Fig. 5.

On the basis of Fig. 5a, for TW10 sample heat-treated at 410 °C for 24 h, it can be concluded that the observed peaks matched the peak positions of orthorhombic γ-TeO_2 and tetragonal α-TeO_2 phases. There is no evidence of the metastable δ-TeO_2 phase due to the transformation of δ-TeO_2 → α-TeO_2. Therefore, for TW10 sample, the formation of the δ-TeO_2 phase was achieved at 390 °C and the transformation of this metastable phase was completed at 410 °C into α-TeO_2, which matches

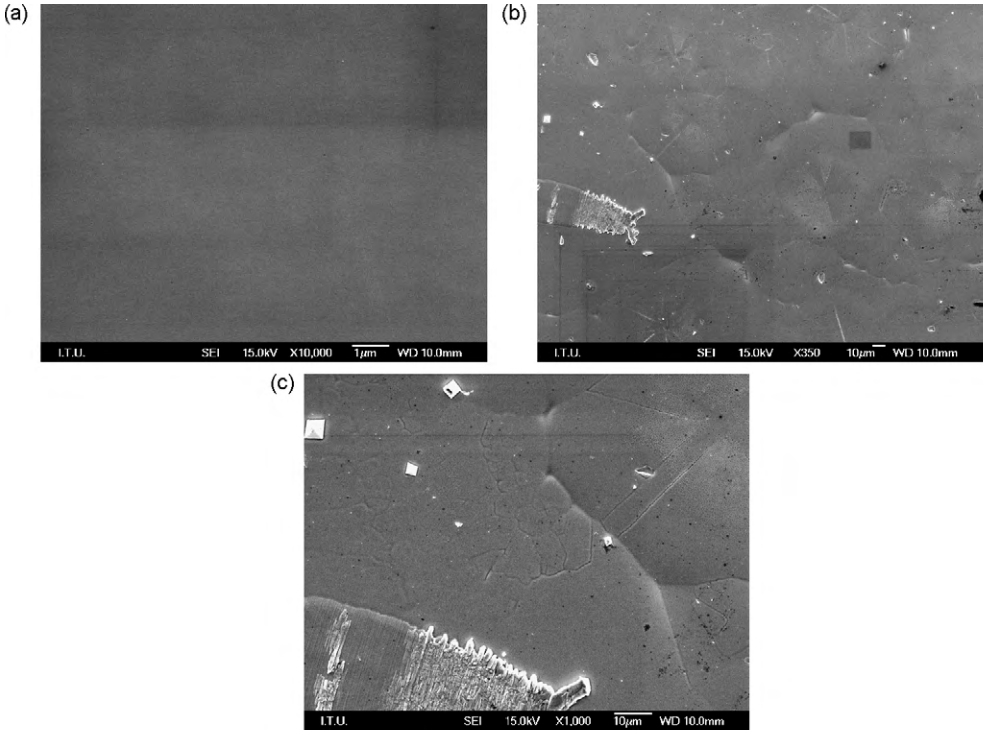

Fig. 6. SEM micrographs of TW10 sample (a) as-cast 10,000×, (b) heat-treated at 390 °C for 24 h, 350× and (c) heat-treated at 390 °C for 24 h, 1000×.

with the results present in the literature.[2,3,6] Blanchandin et al.[2] obtained δ-TeO_2 phase by annealing 5 mol% WO_3 containing glassy samples for 24 h at 350 °C which transforms into the α-TeO_2 phase at 380 °C. In another study, Blanchandin et al.[3] also reported the formation of δ-TeO_2 phase in the TeO_2–Nb_2O_5 system for 5 and 10 mol% Nb_2O_5, at 350 °C and 370 °C, respectively. The transformation of δ-TeO_2 phase was determined at 410 °C for 5 mol% Nb_2O_5 containing sample and at 450 °C for 10 mol% Nb_2O_5 containing sample. Tatar et al.[6] also observed the formation of δ-TeO_2 phase at 420 °C and the transformation of the metastable δ-TeO_2 phase into the stable α-TeO_2 at 560 °C for the TeO_2–CdF_2–WO_3 glass system.

As can be seen in Fig. 5b and c, the observed peak positions for TC10 and TW5C5 samples heat-treated for 24 h at 370 °C and 435 °C, respectively revealed the presence of δ-TeO_2 and γ-TeO_2 phases. However, the formation of α-TeO_2 phase was not detected for CdO containing samples (TC10 and TW5C5) indicating the transformation of δ-TeO_2 was not completed and requires higher temperatures. Therefore, it can be concluded that the addition of CdO into the tellurite glasses, increases the stability range of the δ-TeO_2 phase.

3.3. SEM/EDS investigations

To have a deep understanding on the morphology of the δ-TeO_2 crystalline phase, SEM/EDS investigations were conducted on as-cast samples and heat-treated samples above the first crystallization onset temperature. Fig. 6a–c represents a series of SEM micrographs taken from the outer surface of the as-cast and heat-treated TW10 sample for different magnifications.

As can be seen in Fig. 6a, as-cast TW10 sample revealed no crystallization, proving the glassy nature of the sample. However, TW10 sample heat-treated at 390 °C for 24 h showed the presence of grain-like crystallites on the general structure and the initial formation of centrosymmetric fan-like crystallites with some small white crystallites on the surface (Fig. 6b and c). According to the XRD pattern (see Fig. 4a), the dominant crystalline phase was δ-TeO_2 and γ-TeO_2 formed in the structure as a secondary crystalline phase. Therefore, the grain-like morphology obtained in the SEM micrographs is thought to be due to the formation of δ-TeO_2 phase on the surface. The initiation of centrosymmetric fan-like crystallization on the surface must be due to the formation of the γ-TeO_2 crystalline phase, which was also reported by Ovecoglu et al.[7] for $0.85TeO_2$–$0.15WO_3$ sample heat-treated at 510 °C for 24 h. Besides, EDS spectra taken from the white crystallites varying between 1–2 μm in size on the surface showed that they are TeO_2-rich crystals.

SEM micrographs showing the morphology of as-cast and heat-treated TC10 sample above the first crystallization onset temperature (335 °C) are given in Fig. 7a–c.

Fig. 7a shows that there is no crystallization for the as-cast TC10 sample, which indicates the amorphous structure of the sample. As can be seen from Fig. 7b and c, the micrographs show grain-like crystallites on the surface with some small white crystals. According to the XRD pattern (see Fig. 4b), δ-TeO_2 phase was formed from the glassy matrix, therefore the grain-like crystallites observed in the SEM micrographs must be due to the formation of δ-TeO_2 phase on the surface. Additionally, EDS spectra taken from the white crystallites with the sizes under 1 μm on the surface revealed that they are TeO_2-rich crystals.

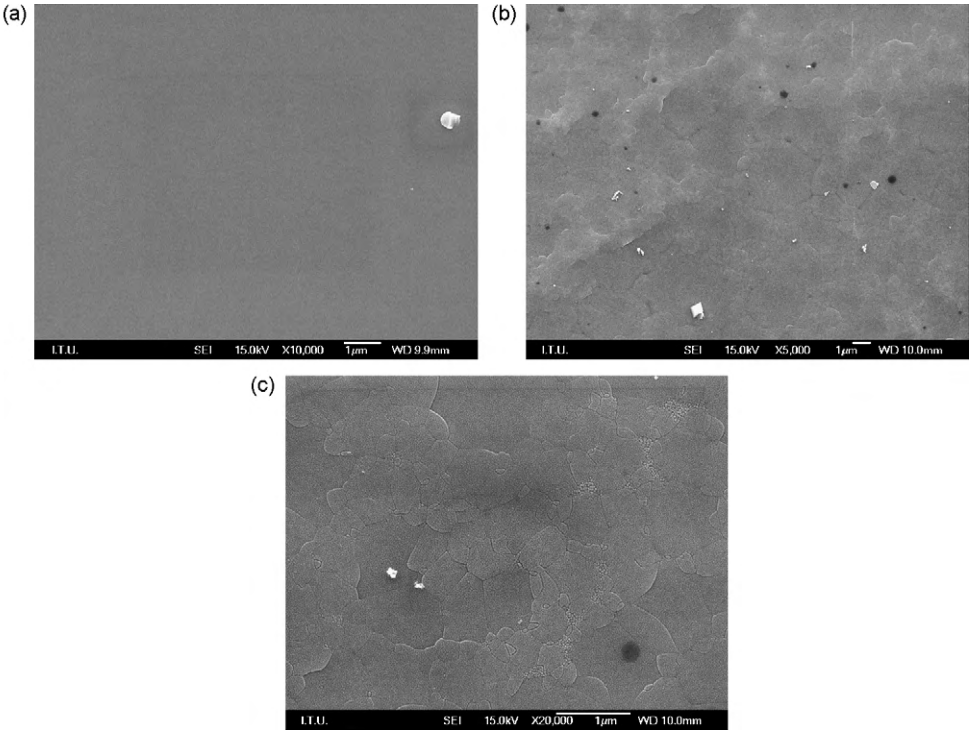

Fig. 7. SEM micrographs of TC10 sample (a) as-cast 10,000×, (b) heat-treated at 335 °C for 24 h, 5000× and (c) heat-treated at 335 °C for 24 h, 20,000×.

Fig. 8a–c shows the SEM micrographs taken from the outer surface of the as-cast and heat-treated TW5C5 sample at 365 °C for different magnifications.

Fig. 8a shows that no crystallization occurs in the as-cast TW5C5 sample, showing the glassy nature of the sample. It can be seen in Fig. 8b and c, the SEM micrographs of TW5C5 sample are similar to the TC10 sample, having grain-like crystallites on the surface and some small white crystals. According to the XRD pattern (see Fig. 4c), δ-TeO_2 phase was formed from the glassy matrix as observed in the TC10 sample. Hence, the grain-like crystallites are thought to be due to the formation of δ-TeO_2 phase on the surface. Also, EDS spectra taken from the white

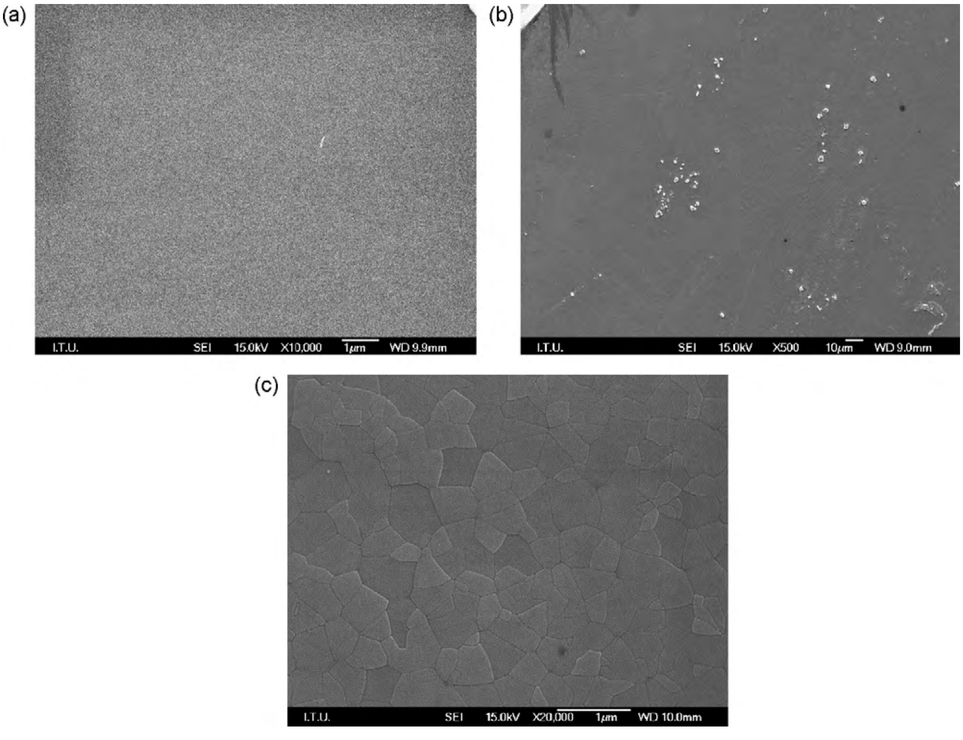

Fig. 8. SEM micrographs of TW5C5 sample (a) as-cast 10,000×, (b) heat-treated at 365 °C for 24 h, 500×, (c) heat-treated at 365 °C for 24 h, 20,000×.

crystallites with the sizes about 1–2 μm on the surface revealed that that they are TeO_2-rich crystals.

4. Conclusions

Thermal, phase and microstructural investigations were realized on the TW10, TC10 and TW5C5 samples in order to characterize the metastable δ-TeO_2 phase in TeO_2-rich part of the binary TeO_2–WO_3, TeO_2–CdO and ternary TeO_2–WO_3–CdO glasses. According to the XRD results, as-cast samples showed amorphous structure, proving the glassy nature of the samples. Therefore, as-cast samples were heat-treated above the first and second crystallization onset temperatures to identify the formation and transformation of the δ-TeO_2 phase. For TW10 sample, both DTA and XRD results showed that the metastable δ-TeO_2 phase forms at 390 °C and transforms into the stable α-TeO_2 form at 410 °C, which is in agreement with the literature. For TC10 and TW5C5 samples, the formation of metastable δ-TeO_2 phase was observed at 335 °C and 365 °C, respectively. The formation of α-TeO_2 phase was not observed for CdO containing samples in the studied temperature interval, showing that the transformation of δ-TeO_2 into α-TeO_2 phase was not completed. δ-TeO_2 phase was detected for the first time in the literature for CdO containing binary and ternary TeO_2 based glasses. The addition of CdO into the tellurite glasses increased the stability range of the δ-TeO_2 phase and in CdO containing samples it was also proved that the formation of δ-TeO_2 phase occurred in a wider compositional range. SEM images of the δ-TeO_2 phase were taken, revealing the formation of δ-TeO_2 phase on the surface as grain-like crystallites.

Acknowledgements

The authors gratefully acknowledge The Scientific & Technological Research Council of Turkey (TUBITAK) for the financial support under the project numbered 108M077.

References

1. El-Mallawany RAH. *Tellurite glasses handbook*. Boca Raton/London/New York/Washington, DC: CRC Press; 2002.
2. Blanchandin S, Marchet P, Thomas P, Champarnaud-Mesjard JC, Frit B, Chagraoui A. New investigations within the TeO_2–WO_3 system: phase equilibrium diagram and glass crystallization. *Journal of Materials Science* 1999;**34**:4285–92.
3. Blanchandin S, Thomas P, Marchet P, Champarnaud-Mesjard JC, Frit B. Equilibrium and nonequilibrium phase diagram within the TeO_2-rich part of the TeO_2–Nb_2O_5 system. *Journal of Materials Chemistry* 1999;**9**: 1785–8.
4. Mirgorodsky AP, Merle-Mejean T, Champarnaud JC, Thomas P, Frit B. Dynamics and structure of TeO_2 polymorphs: model treatment of paratellurite and tellurite; Raman scattering evidence for new γ- and δ-phases. *Journal of Physics and Chemistry of Solids* 2000;**61**:501–9.
5. Noguera O, Merle-Mejean T, Mirgorodsky AP, Smirnov MB, Thomas P, Champarnaud JC. Vibrational and structural properties of glass and crystalline phases of TeO_2. *Journal of Non-Crystalline Solids* 2003;**330**: 50–60.
6. Tatar D, Özen G, Erim FB, Öveçoğlu ML. Raman characterizations and structural properties of the binary TeO_2–WO_3, TeO_2–CdF_2 and ternary TeO_2–CdF_2–WO_3 glasses. *Journal of Raman Spectroscopy* 2009, doi:10.1002/jrs.2519.
7. Öveçoğlu ML, Özen G, Cenk S. Microstructural characterization and crystallization behavior of $(1-x)TeO_2$–xWO_3 ($x = 0.15$, 0. 25, 0. 3 mol) glasses. *Journal of the European Ceramic Society* 2006;**26**:1149–58.